Hindawi
Journal of Mathematics
Volume 2023, Article ID 4833683, 12 pages
https://doi.org/10.1155/2023/4833683

Research Article

Analysis of Zigzag and Rhombic Benzenoid Systems via Irregularity Indices

Muhammad Awais,[1,2] Zulfiqar Ahmed,[1] Waseem Khalid,[1] and Ebenezer Bonyah[3]

[1]*School of Engineering and Applied Sciences, Department of Computer Science, GIFT University, Gujranwala, Pakistan*
[2]*School of Mathematics and Statistics, Southwest University, Chongqing, China*
[3]*Faculty of Applied Sciences and Mathematics Education, AAMUSTED, Kumasi, Ghana*

Correspondence should be addressed to Ebenezer Bonyah; ebonyah@uew.edu.gh

Received 7 August 2022; Revised 15 March 2023; Accepted 20 March 2023; Published 26 May 2023

Academic Editor: Tareq Al-shami

Topological indices are numerical quantities associated with the molecular graph of a chemical structure. These indices are used to predict various properties of chemical structures. Imbalance-based analysis is an advanced technique used for chemical compounds with irregular characteristics. The molecular graphs of zigzag benzenoid systems (Z_p) and rhombic benzenoid systems (R_p) are inherently irregular. Therefore, applying the imbalance technique to these molecular structures plays an important role in predicting different properties. In this paper, we calculate sixteen irregularity indices for both Z_p and R_p systems. By examining these indices, we aim to provide insights into the properties of these structures and ultimately contribute to a deeper understanding of the field.

1. Introduction

Graph theory is a branch of mathematics that deals with the study of graphs and their properties. Graphs are a type of mathematical structure that consists of nodes (also called vertices) and edges, which represent connections between the nodes. Graph theory has many applications, including computer science, biology, social network analysis, and more. One of the fundamental concepts in graph theory is the idea of a path, which is a sequence of edges connecting two nodes (see [1, 2]). Another important concept is the degree of a node, which refers to the number of edges connected to that node. Graph theory also includes the study of graph coloring, which involves assigning colors to the nodes of a graph in such a way that adjacent nodes have different colors. The study of graph theory has led to many important results and discoveries and continues to be an active area of research (see [3]).

In this paper, all graphs under consideration are finite, simple, and undirected. Let G be a graph with vertex set V and edge set E. The degree of a vertex u in G is denoted by d_u and is defined as the number of edges incident to vertex u. In other words, d_u is the number of vertices adjacent to vertex u in G. The distance between any two vertices in G is defined as the length of the shortest path between them. Therefore, the degree of a vertex u can also be defined as the number of vertices at distance one from u. This notion of degree is fundamental to the study of graphs and plays a key role in many of their properties and applications.

In mathematical chemistry, the study of the graphical structure of chemical compounds allows researchers to predict important properties without performing experiments in a laboratory. This field of study is known as chemical graph theory [4, 5]. A simple graph is defined as a graph without loops or multiple edges. In chemical graph theory, atoms are represented by vertices (or nodes) and chemical bonds are represented by edges (or lines). The degree of a vertex is defined as the number of edges that are incident to it. The study of topological indices in chemical graph theory began with the Wiener index in 1947, followed by the Zagreb indices, which were introduced due to the vast number of applications of the Wiener index [6]. The

mathematical formulas for the first and second Zagreb indices are given by

$$M_1(G) = \sum_{uv \in E(G)} (d_u + d_v),$$
$$M_2(G) = \sum_{uv \in E(G)} (d_u \times d_v). \quad (1)$$

In addition to the Wiener and Zagreb indices, many other types of indices have been introduced to analyze the topology of different chemical structures [7, 8]. To measure the irregularities present in a chemical structure, irregularity indices have been introduced [9, 10]. These indices provide valuable insights into the properties of chemical structures and can help researchers make predictions and discoveries in the field of mathematical chemistry.

An irregularity measure index is a mathematical index that takes a value of either zero or greater than zero and is used to measure the irregularities present in a chemical structure [11]. These indices are calculated based on the degree of vertices, which is a fundamental property of the chemical graph. Table 1 presents the mathematical formulas for these irregularity measure indices, which can be used to predict various properties of the chemical compounds under consideration. However, the interpretation and analysis of these indices can be complex, and their application requires a deep understanding of the underlying principles of chemical graph theory. Nonetheless, they provide valuable insights into the properties and behavior of the molecules and can aid in the discovery of new compounds with specific properties. Therefore, the study of irregularity measure indices is crucial for researchers in the field of mathematical chemistry.

For a detailed background on these irregularity measure indices, we refer readers to the literature [13–16]. These studies provide a comprehensive overview of the theory and application of irregularity indices in chemical graph theory and cover a wide range of topics such as their mathematical properties, algorithmic complexity, and relationship with other topological indices. The works also provide examples of their application in predicting various properties of chemical compounds, such as boiling points, melting points, and refractive indices. Therefore, a thorough understanding of these studies is essential for researchers interested in exploring the potential of irregularity indices in the field of mathematical chemistry.

Benzenoid systems have significant importance in theoretical chemistry due to their natural graph representation of benzenoid hydrocarbons [17]. In a hexagonal system, there exists a vertex that belongs to three hexagons, which is known as the internal vertex of the hexagonal system [18]. Benzenoid hydrocarbons are commonly found in our surroundings, minerals, and food and are also produced as byproducts in certain reactions, with a wide range of applications in chemical synthesis [19]. However, despite their widespread use, benzenoid hydrocarbons are known to be pollutants and carcinogenic. Benzenoid systems are essentially hydrogen-deprived benzenoid hydrocarbons [20].

The authors in [21] emphasized the importance of the three-dimensional distribution of benzene. More information about this repetitive surface can be found in [22, 23]. The structure needed to be connected as a three-dimensional solid carbon; however, to our knowledge, no such sequence has been considered for such a purpose. This goal was aimed at raising the awareness of researchers towards the atomic recognition of such friendly concepts in carbon nanoscience [24, 25].

The aim of this present work is to comprehensively study the topological properties of zigzag and rhombic benzenoid systems, which are two important families of benzenoid systems. To achieve this goal, we start by sketching the graphs of these systems and determining the number of vertices and edges in each graph. We then classify the edges into different classes based on the degrees of the end vertices. Using these classifications, we calculate 16 irregularity measures for each system. Our findings provide valuable insights into the topological behavior of these systems.

2. Results

2.1. Irregularity Indices for Zigzag Benzenoid System Z_p. Figure 1 shows the graph Z_p, which consists of p rows, with each row consisting of two hexagonal units sharing one common edge. The first row of Z_p contains eleven edges, while the second row has twenty-one edges. Continuing in the same pattern, we can deduce that Z_p has $10p + 1$ edges and $8p + 2$ vertices. There are three types of edges present in Z_p, namely, (2, 2), (2, 3), and (3, 3). We can partition the edges into three sets $\mathscr{P}_1$, $\mathscr{P}_2$, and $\mathscr{P}_3$, where $\mathscr{P}_1$ has $2p + 4$ edges, $\mathscr{P}_2$ has $4p$ edges, and $\mathscr{P}_3$ has $4p - 3$ edges. These edge partitions are denoted as $\mathscr{P} = \mathscr{P}_1 + \mathscr{P}_2 + \mathscr{P}_3$. These observations provide useful information about the structure of Zp and can aid researchers in understanding the topological properties of this important family of benzenoid systems. Table 2 displays the three edge partitions $\mathscr{P}1$, $\mathscr{P}2$, and $\mathscr{P}3$ of the hexagonal system Z_p.

Theorem 1. *Consider the graph G corresponding to Z_p. It can be observed that*

(1) $VAR(G) = 2(2p^2 + p - 1)/(4p + 1)^2$.
(2) $AL(G) = 4p$.
(3) $IR1(G) = 2(2p^2 + p - 1)/4p + 1$.
(4) $IR2(G) = \sqrt{68p - 11/10p + 1} - 2(10p + 1)/8p + 2$.
(5) $IRF(G) = 4p$.
(6) $IRFW(G) = 4p/68p - 11$.
(7) $IRA(G) = 2/3(5 - 2\sqrt{6})p$.
(8) $IRB(G) = (20 - 8\sqrt{6})p$.
(9) $IRC(G) = 2(8\sqrt{6}$
$p^2 + 2\sqrt{6}\,p - 18p^2 - 4p - 1)/(10p + 1)(4p + 1)$.
(10) $IRDIF(G) = 3.33p$.
(11) $IRL(G) = 1.6216p$.
(12) $IRLU(G) = 2p$.
(13) $IRLF(G) = 1.6329$.

Table 1: Definitions of irregularities [12].

Irregularity index	Mathematical form
VAR	$\sum_{u\epsilon V}(d_u - (2m/n))^2 = M_1(G)/n - (2m/n)^2$
AL	$\sum_{uv\epsilon E(G)}\lvert d_u - d_v\rvert$
IR1	$\sum_{u\epsilon V}(d_u)^3 - (2m/n)\sum_{u\epsilon V}(d_u)^2 = F(G) - (2m/n)M_1(G)$
IR2	$\sqrt{\sum_{uv\epsilon E(G)} d_u d_v/m} - (2m/n) = \sqrt{(M_2(G)/m)} - (2m/n)$
IRF	$\sum_{uv\epsilon E(G)}(d_u - d_v)^2 = F(G) - 2M_2(G)$
IRFW	$\mathrm{IRF}(G)/M_2(G)$
IRA	$\sum_{uv\epsilon E(G)}(d_u^{-(1/2)} - d_v^{-(1/2)})^2 = n - 2R(G)$
IRB	$\sum_{uv\epsilon E(G)}(d_u^{-(1/2)} - d_v^{-(1/2)})^2 = M_1(G) - 2\mathrm{RR}(G)$
IRC	$\sum_{uv\epsilon E(G)}\sqrt{d_u d_v}/m - (2m/n) = \mathrm{RR}(G)/m - (2m/n)$
IRDIF	$\sum_{uv\epsilon E(G)}\lvert d_u/d_v - d_v/d_u\rvert = \sum_{i<j} m_{i,j}(j/i - i/j)$
IRL	$\sum_{uv\epsilon E(G)}\lvert \mathrm{lnd}_u - \mathrm{lnd}_v\rvert = \sum_{i<j} m_{i,j}\ln(j/i)$
IRLU	$\sum_{uv\epsilon E(G)}\lvert d_u - d_v/\min(d_u, d_v)\rvert = \sum_{i<j} m_{i,j}\ln(j - i/i)$
IRLF	$\sum_{uv\epsilon E(G)}\lvert d_u - d_v/\sqrt{(d_u d_v)}\rvert = \sum_{i<j} m_{i,j}(j - i/\sqrt{ij})$
IRLA	$2\sum_{uv\epsilon E(G)}\lvert d_u - d_v/(d_u + d_v)\rvert = 2\sum_{i<j} m_{i,j}(j - i/i + j)$
IRDI	$\sum_{uv\epsilon E(G)}\ln 1 + \lvert d_u - d_v\rvert = \sum_{i<j} m_{i,j}\ln(i + j - 1)$
IRGA	$\sum_{uv\epsilon E(G)}\ln\lvert d_u + d_v/2\sqrt{d_u d_v}\rvert = \sum_{i<j} m_{i,j}(i + j/2\sqrt{ij})$

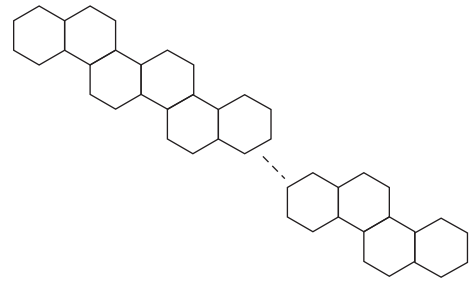

Figure 1: Molecular graph of Z_p.

Table 2: $E(Z_p)$.

$\mathscr{P}$	(d_u, d_v)	Frequency
$\mathscr{P}_1$	(2, 2)	$2p + 4$
$\mathscr{P}_2$	(2, 3)	$4p$
$\mathscr{P}_3$	(3, 3)	$4p - 3$

(14) $IRLA(G) = 1.6p$.

(15) $IRD1(G) = 2.7724p$.

(16) $IRGA(G) = 0.0816p$.

Proof. We can obtain our desired results by utilizing the mathematical formulas for irregularity indices given in Table 1 and the edge partitions of Z_p presented in Table 2.

$$\begin{aligned}
\mathrm{VAR}(G) &= \sum_{u\epsilon V}\left(d_u - \frac{2m}{n}\right)^2 = \frac{M_1(G)}{n} - \left(\frac{2m}{n}\right)^2 \\
&= \left(\frac{52p-2}{8p+2}\right) - \left(\frac{2(10p+1)}{8p+2}\right)^2 \\
&= \frac{2\left(2p^2+p-1\right)}{(4p+1)^2}.
\end{aligned}$$

$$\begin{aligned}
\mathrm{AL}(G) &= \sum_{uv\epsilon E(G)} \left|d_u - d_v\right| \\
&= |2-2|(2p+4) + |2-3|(4p) + |3-3|(4p-3) \\
&= 4p.
\end{aligned}$$

$$\begin{aligned}
\mathrm{IR1}(G) &= \sum_{u\epsilon V} d_u^3 - \frac{2m}{n}\sum_{u\epsilon V} d_u^2 = F(G) - \left(\frac{2m}{n}\right)M_1(G) \\
&= (140p-22) - \frac{2(10p+1)}{8p+2}(52p-2) \\
&= \frac{20\left(2p^2+p-1\right)}{4p+1}.
\end{aligned}$$

$$\begin{aligned}
\mathrm{IR2}(G) &= \sqrt{\frac{\sum_{uv\epsilon E(G)} d_u d_v}{m}} - \frac{2m}{n} = \sqrt{\frac{M_2(G)}{m}} - \frac{2m}{n} \\
&= \sqrt{\frac{68p-11}{10p+1}} - \frac{2(10p+1)}{8p+2} \\
&= \sqrt{\frac{68p-11}{10p+1}} - \frac{2(10p+1)}{8p+2}.
\end{aligned}$$

$$\begin{aligned}
\mathrm{IRF}(G) &= \sum_{uv\epsilon E(G)} \left(d_u - d_v\right)^2 \\
&= (2-2)^2(2p+4) + (2-3)^2(4p) + (3-3)^2(4p-3) \\
&= 4p.
\end{aligned}$$

$$\begin{aligned}
\mathrm{IRFW}(G) &= \frac{\mathrm{IRF}(G)}{M_2(G)} \\
&= \frac{4p}{68p-11}.
\end{aligned}$$

$$\begin{aligned}
\mathrm{IRA}(G) &= \sum_{uv\epsilon E(G)} \left(d_u^{-(1/2)} - d_v^{-(1/2)}\right)^2 = n - 2R(G) \\
&= (8p+2) - 2\left(\frac{7}{3}p + 1 + \frac{2}{3}\sqrt{2}\,p\right) \\
&= \frac{2}{3}\left(5 - 2\sqrt{6}\right)p.
\end{aligned}$$

$$\mathrm{IRB}(G) = \sum_{uv\epsilon E(G)} \left(d_u^{-(1/2)} - d_v^{-(1/2)}\right)^2 = M_1(G) - 2\mathrm{RR}(G)$$

$$
\begin{aligned}
&= (52p - 2) - 2(16p - 1 + 4\sqrt{6}\,p)\\
&= (20 - 8\sqrt{6})p.\\
\mathrm{IRC}(G) &= \frac{\sum_{uv\in E(G)}\sqrt{d_u d_v}}{m} - \frac{2m}{n} = \frac{RR(G)}{m} - \frac{2m}{n}\\
&= \frac{16p - 1 + 4\sqrt{6}p}{10p + 1} - \frac{2(10p + 1)}{8p + 2}\\
&= \frac{2\left(8\sqrt{6}\,p^2 + 2\sqrt{6}\,p - 18p^2 - 4p - 1\right)}{(10p + 1)(4p + 1)}.\\
\mathrm{IRDIF}(G) &= \sum_{uv\in E(G)}\left|\frac{d_u}{d_v} - \frac{d_v}{d_u}\right|\\
&= \left|\frac{2}{2} - \frac{2}{2}\right|(2p + 4) + \left|\frac{2}{3} - \frac{3}{2}\right|(4p) + \left|\frac{3}{3} - \frac{3}{3}\right|(4p - 3)\\
&= 3.33p.\\
\mathrm{IRL}(G) &= \sum_{uv\in E(G)}\left|\ln d_u - \ln d_v\right|\\
&= |\ln 2 - \ln 2|(2p + 4) + |\ln 2 - \ln 3|(4p) + |\ln 3 - \ln 3|(4p - 3)\\
&= 1.6216p.\\
\mathrm{IRLU}(G) &= \sum_{uv\in E(G)}\frac{|d_u - d_v|}{\min(d_u, d_v)}\\
&= \frac{|2 - 2|}{2}(2p + 4) + \frac{|2 - 3|}{2}(4p) + \frac{|3 - 3|}{3}(4p - 3)\\
&= 2p.\\
\mathrm{IRLF}(G) &= \sum_{uv\in E(G)}\frac{|d_u - d_v|}{\sqrt{d_u.d_v}}\\
&= \frac{|2 - 2|}{\sqrt{4}}(2p + 4) + \frac{|2 - 3|}{\sqrt{6}}(4p) + \frac{|3 - 3|}{\sqrt{9}}(4p - 3)\\
&= 1.6329.\\
\mathrm{IRLA}(G) &= \sum_{uv\in E(G)}2\frac{|d_u - d_v|}{(d_u + d_v)}\\
&= 2\frac{|2 - 2|}{4}(2p + 4) + 2\frac{|2 - 3|}{5}(4p) + 2\frac{|3 - 3|}{6}(4p - 3)\\
&= 1.6p.\\
\mathrm{IRD1}(G) &= \sum_{uv\in E(G)}\ln\left\{1 + \left|d_u - d_v\right|\right\}\\
&= \ln\{1 + |2 - 2|\}(2p + 4) + \ln\{1 + |2 - 3|\}(4p) + \ln\{1 + |3 - 3|\}(4p - 3)\\
&= 2.7724p.\\
\mathrm{IRGA}(G) &= \sum_{uv\in E(G)}\ln\left(\frac{d_u + d_v}{2\sqrt{d_u d_v}}\right)\\
&= \ln\left(\frac{2 + 2}{2\sqrt{2\times 2}}\right)(2p + 4) + \ln\left(\frac{2 + 3}{2\sqrt{2\times 3}}\right)(4p) + \ln\left(\frac{3 + 3}{2\sqrt{3\times 3}}\right)(4p - 3)\\
&= 0.0816p.
\end{aligned}
\tag{2}
$$

□

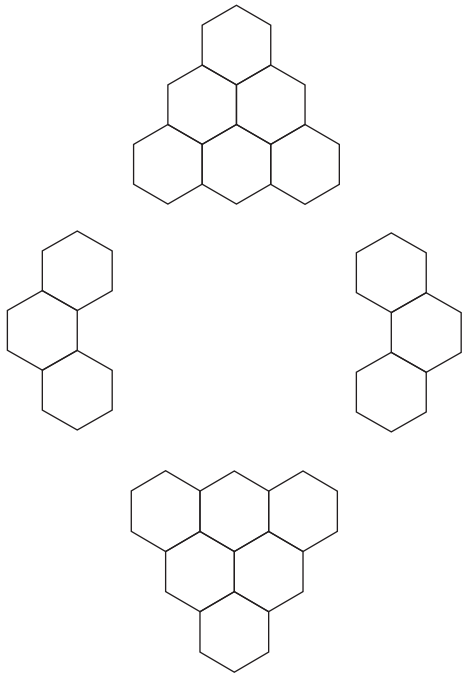

Figure 2: Molecular graph of R_p.

Table 3: $E(R_p)$.

(d_u, d_v)	Frequency
(2, 2)	6
(2, 3)	$8p - 8$
(3, 3)	$3p^2 - 4p + 1$

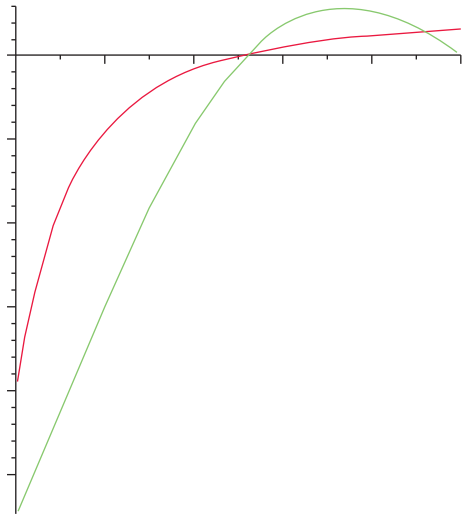

Figure 3: Plots of VAR index.

2.2. Irregularity Indices for Rhombic Benzenoid System R_p. The graph of R_p is shown in Figure 2. We can see that R_p contains three types of edges, namely, (2, 2), (2, 3), and (3, 3). The edge set of R_p can be partitioned into three

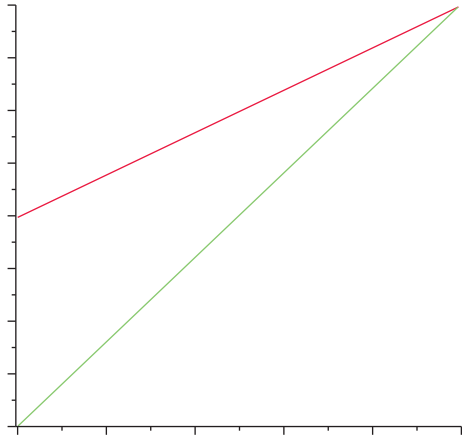

Figure 4: Plots of AL index.

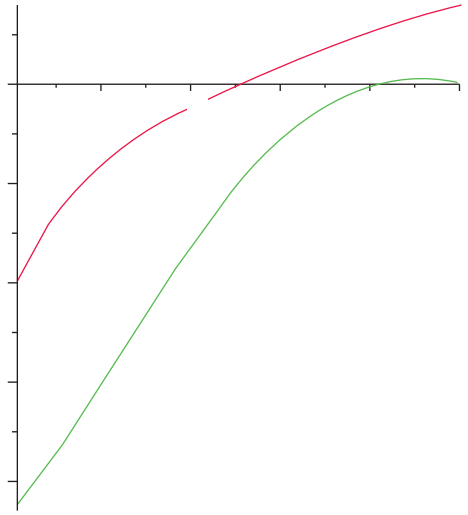

Figure 5: Plots of IR1 index.

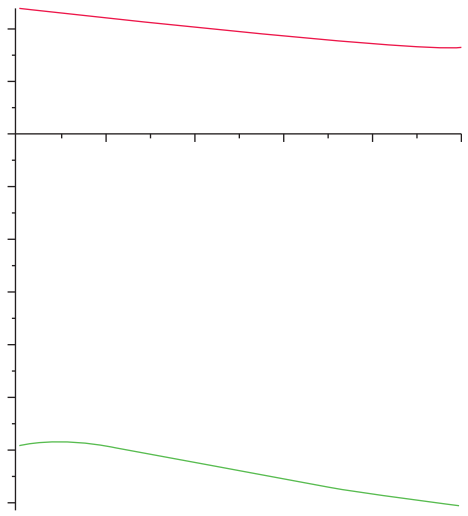

Figure 6: Plots of IR2 index.

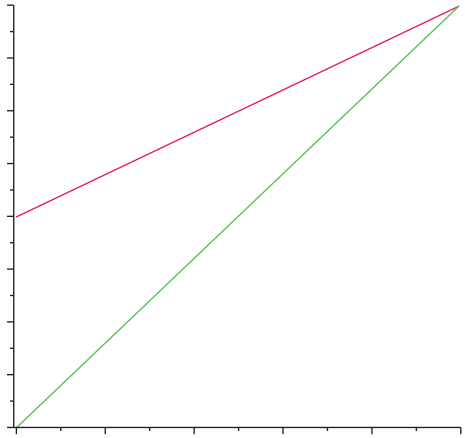

Figure 7: Plots of IRF index.

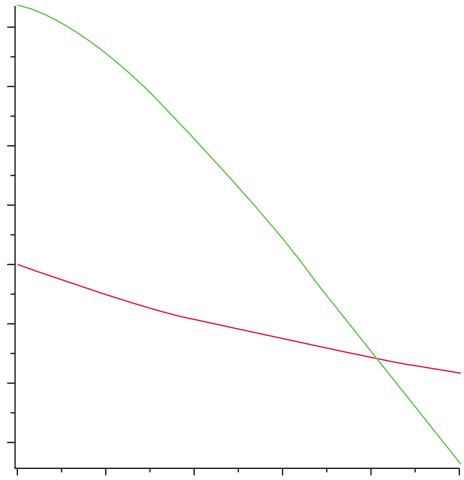

Figure 8: Plots of IRFW index.

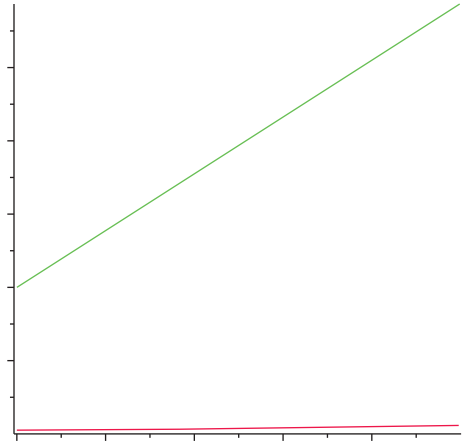

Figure 9: Plots of IRA index.

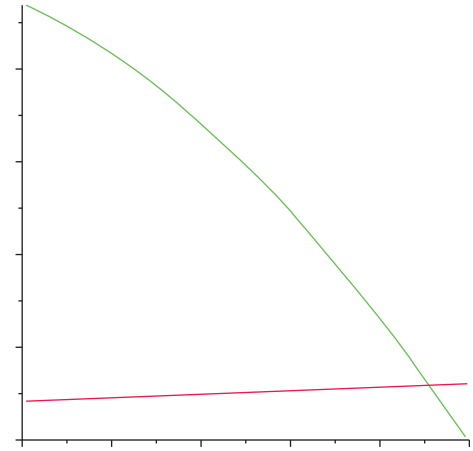

Figure 10: Plots of IRB index.

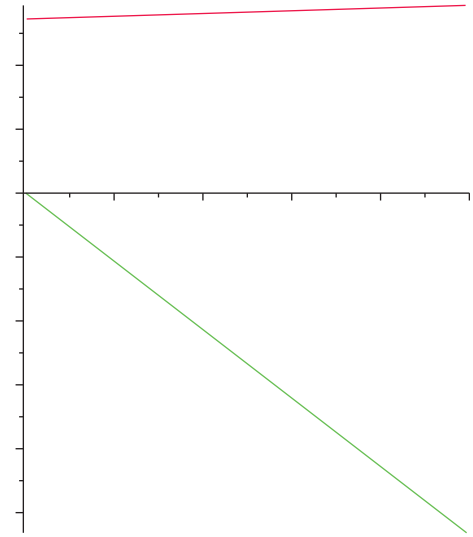

Figure 11: Plots of IRC index.

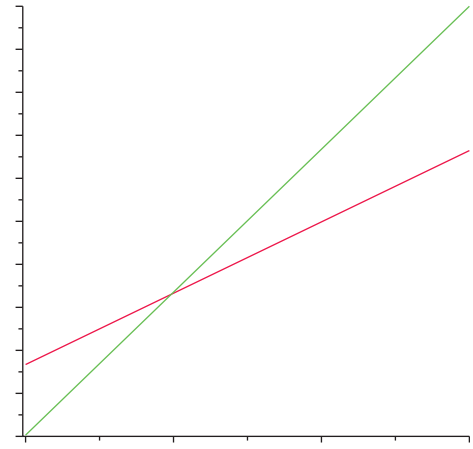

Figure 12: Plots of IRDIF index.

subsets, denoted by $\mathscr{P}_1$, $\mathscr{P}_2$, and $\mathscr{P}_3$, based on the types of edges.

It can be shown that the total number of edges in R_p is $32pq - 2p - 2q$. This result can be obtained by counting the number of edges in each row of the graph and summing over all rows. Specifically, the number of edges in the ith row is $8(p + q - i) + 4$, for $1 \le i \le p + q - 1$, and the number of edges in the last row is $4p + 4q - 4$. Summing over all rows, we obtain the total number of edges as $32pq - 2p - 2q$,

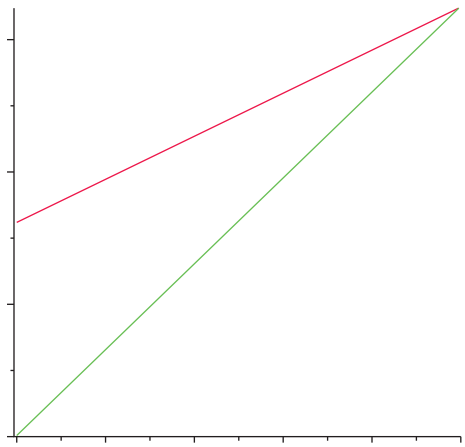

Figure 13: Plots of IRL index.

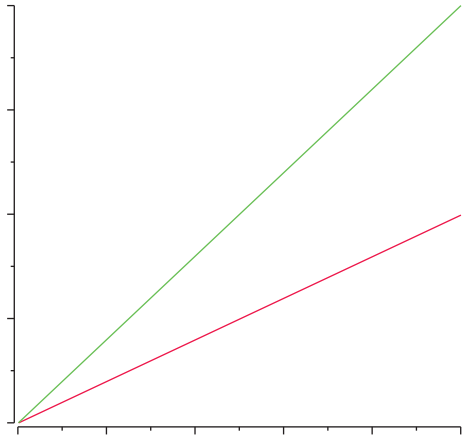

Figure 14: Plots of IRLU index.

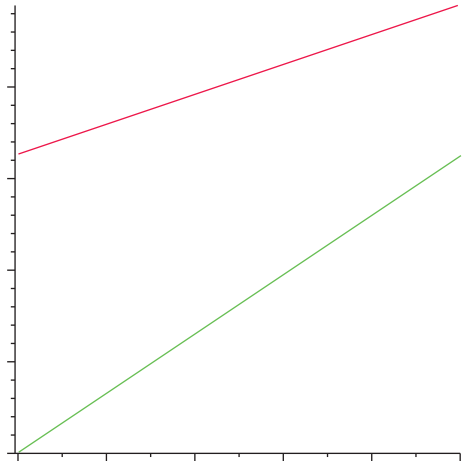

Figure 15: Plots of IRLF index.

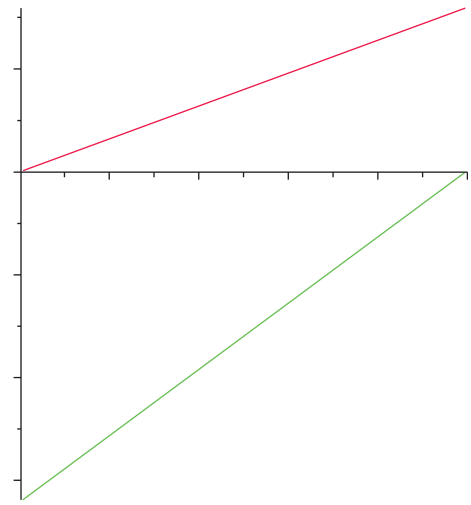

Figure 16: Plots of IRLA index.

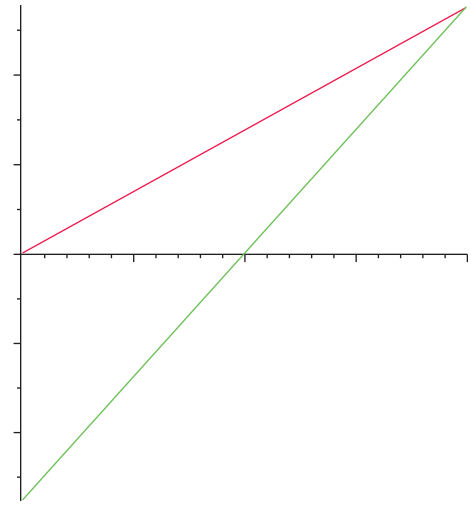

Figure 17: Plots of IRD1 index.

which can be verified by direct calculation. Table 3 presents the edge partition of R_p. The first column shows the types of edges, i.e., (2, 2), (2, 3), and (3, 3), and the second column shows the number of edges of each type.

Theorem 2. *Consider the graph G corresponding to the rhombic benzenoid system R_p. Then, we have*

(1) $VAR(G) = -(16p^3 - 3p^2 - 24p + 11)/(p^2 + 2)^2$.

(2) $AL(G) = 8p - 8$.

(3) $IR1(G) = -2(44p^3 - 27p^2 - 60p + 43)/p^2 + 2$.

(4) $IR2(G) = \sqrt{7p^2 + 12p - 15/2p^2 + 4} - 2(3p^2 + 4p - 1)/2p^2 + 4$.

(5) $IRF(G) = 8p - 8$.

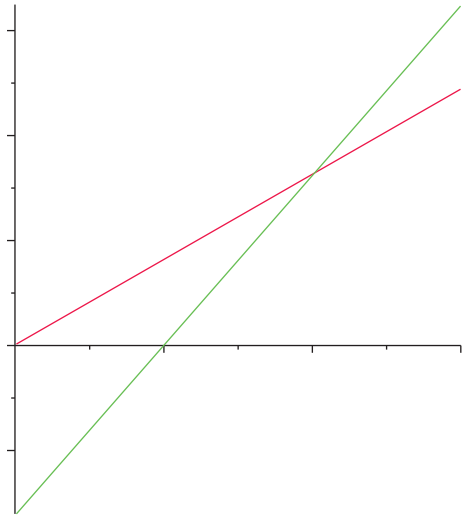

Figure 18: Plots of IRGA index.

(6) $IRFW(G) = 8p - 8/27p^2 + 12p - 15$.

(7) $IRA(G) = 8/3(-1 + \sqrt{6} - \sqrt{6}p + p)$.

(8) $IRB(G) = -10p^2 + 40p - 40 - 16\sqrt{6}p + 16\sqrt{6}$.

(9) $IRC(G) = 8\sqrt{6}p^3 - 8\sqrt{6}p^2 - 36p^3 + 16\sqrt{6}p + 23p^2 - 16\sqrt{6} - 16p + 29/(3p^2 + 4p - 1)(p^2 + 2)$.

(10) $IRDIF(G) = 2.66p - 2.66$.

(11) $IRL(G) = 3.2432p - 3.2432$.

(12) $IRLU(G) = 4p - 4$.

(13) $IRLF(G) = 3.2656p - 3.2656$.

(14) $IRLA(G) = 3.2p - 3.2$.

(15) $IRD1(G) = 5.5448p - 5.5448$.

(16) $IRGA(G) = 0.1632p - 0.1632$.

Proof. Using the mathematical formulas of irregularity indices given in Table 1 and the edge partition of the rhombic benzenoid system R_p given in Table 3, we can perform the following computations to obtain our desired results.

$$\begin{aligned}
\mathrm{VAR}(G) &= \sum_{u\epsilon V}\left(d_u - \frac{2m}{n}\right)^2 = \frac{M_1(G)}{n} - \left(\frac{2m}{n}\right)^2 \\
&= \left(\frac{18p^2 + 16p - 10}{2p^2 + 4}\right) - \left(\frac{2\left(3p^2 + 4p - 1\right)}{2p^2 + 4}\right)^2 \\
&= -\frac{16p^3 - 3p^2 - 24p + 11}{\left(p^2 + 2\right)^2}.
\end{aligned}$$

$$\begin{aligned}
\mathrm{AL}(G) &= \sum_{uv\epsilon E(G)} \left|d_u - d_v\right| \\
&= |2 - 2|(6) + |2 - 3|(8p - 8) + |3 - 3|\left(3p^2 - 4p + 1\right) \\
&= 8p - 8.
\end{aligned}$$

$$\begin{aligned}
\mathrm{IR1}(G) &= \sum_{u\epsilon V} d_u^3 - \frac{2m}{n}\sum_{u\epsilon V} d_u^2 = F(G) - \left(\frac{2m}{n}\right)M_1(G) \\
&= \left(54p^2 + 32p - 38\right) - \frac{2\left(3p^2 + 4p - 1\right)}{2p^2 + 4}\left(18p^2 + 16p - 10\right) \\
&= -\frac{2\left(44p^3 - 27p^2 - 60p + 43\right)}{p^2 + 2}.
\end{aligned}$$

$$\begin{aligned}
\mathrm{IR2}(G) &= \sqrt{\frac{\sum_{uv\epsilon E(G)} d_u d_v}{m}} - \frac{2m}{n} = \sqrt{\frac{M_2(G)}{m}} - \frac{2m}{n} \\
&= \sqrt{\frac{7p^2 + 12p - 15}{2p^2 + 4}} - \frac{2\left(3p^2 + 4p - 1\right)}{2p^2 + 4}.
\end{aligned}$$

$$\begin{aligned}
\mathrm{IRF}(G) &= \sum_{uv\epsilon E(G)} (d_u - d_v)^2 \\
&= (2-2)^2(6) + (2-3)^2(8p-8) + (3-3)^2\left(3p^2 - 4p + 1\right) \\
&= 8p - 8. \\
\mathrm{IRFW}(G) &= \frac{\mathrm{IRF}(G)}{M_2(G)} \\
&= \frac{8p-8}{27p^2 + 12p - 15}. \\
\mathrm{IRA}(G) &= \sum_{uv\epsilon E(G)} \left(d_u^{-1/2} - d_v^{-1/2}\right)^2 = n - 2R(G) \\
&= \left(2p^2 + 4\right) - 2\left(\frac{10}{3} + \frac{1}{6}\sqrt{6}\,(8p-8) + p^2 - \frac{4}{3}p\right) \\
&= \frac{8}{3}\left(-1 + \sqrt{6} - \sqrt{6}\,p + p\right). \\
\mathrm{IRB}(G) &= \sum_{uv\epsilon E(G)} \left(d_u^{1/2} - d_v^{1/2}\right)^2 = M_1(G) - 2\mathrm{RR}(G) \\
&= \left(8p^2 + 16p - 10\right) - 2\left(8\sqrt{6}\,p + 9p^2 - 8\sqrt{6} - 12p + 15\right) \\
&= -10p^2 + 40p - 40 - 16\sqrt{6}p + 16\sqrt{6}. \\
\mathrm{IRC}(G) &= \frac{\sum_{uv\epsilon E(G)} \sqrt{d_u d_v}}{m} - \frac{2m}{n} = \frac{\mathrm{RR}(G)}{m} - \frac{2m}{n} \\
&= \frac{8\sqrt{6}p^3 - 8\sqrt{6}p^2 - 36p^3 + 16\sqrt{6}p + 23p^2 - 16\sqrt{6} - 16p + 29}{\left(3p^2 + 4p - 1\right)\left(p^2 + 2\right)}. \\
\mathrm{IRDIF}(G) &= \sum_{uv\epsilon E(G)} \left|\frac{d_u}{d_v} - \frac{d_v}{d_u}\right| \\
&= \left|\frac{2}{2} - \frac{2}{2}\right|(6) + \left|\frac{2}{3} - \frac{3}{2}\right|(8p-8) + \left|\frac{3}{3} - \frac{3}{3}\right|\left(3p^2 - 4p + 1\right) \\
&= 2.66p - 2.66. \\
\mathrm{IRL}(G) &= \sum_{uv\epsilon E(G)} \left|\ln d_u - \ln d_v\right| \\
&= |\ln 2 - \ln 2|(6) + |\ln 2 - \ln 3|(8p-8) + |\ln 3 - \ln 3|\left(3p^2 - 4p + 1\right) \\
&= 3.2432p - 3.2432. \\
\mathrm{IRLU}(G) &= \sum_{uv\epsilon E(G)} \frac{\left|d_u - d_v\right|}{\min\left(d_u, d_v\right)} \\
&= \frac{|2-2|}{2}(6) + \frac{|2-3|}{2}(8p-8) + \frac{|3-3|}{3}\left(3p^2 - 4p + 1\right) \\
&= 4p - 4. \\
\mathrm{IRLF}(G) &= \sum_{uv\epsilon E(G)} \frac{\left|d_u - d_v\right|}{\sqrt{d_u . d_v}} \\
&= \frac{|2-2|}{\sqrt{4}}(6) + \frac{|2-3|}{\sqrt{6}}(8p-8) + \frac{|3-3|}{\sqrt{9}}\left(3p^2 - 4p + 1\right) \\
&= 3.2656p - 3.2656. \\
\mathrm{IRLA}(G) &= \sum_{uv\epsilon E(G)} 2\frac{\left|d_u - d_v\right|}{\left(d_u + d_v\right)}
\end{aligned}$$

$$
\begin{aligned}
&= 2\frac{|2-2|}{4}(6) + 2\frac{|2-3|}{5}(8p-8) + 2\frac{|3-3|}{6}\left(3p^2-4p+1\right)\\
&= 3.2p - 3.2.\\
\mathrm{IRD1}(G) &= \sum_{uv\in E(G)} \ln\left\{1+\left|d_u - d_v\right|\right\}\\
&= \ln\{1+|2-2|\}(6) + \ln\{1+|2-3|\}(8p-8) + \ln\{1+|3-3|\}\left(3p^2-4p+1\right)\\
&= 5.5448p - 5.5448.\\
\mathrm{IRGA}(G) &= \sum_{uv\in E(G)} \ln\left(\frac{d_u+d_v}{2\sqrt{d_u d_v}}\right)\\
&= \ln\left(\frac{2+2}{2\sqrt{2\times 2}}\right)(6) + \ln\left(\frac{2+3}{2\sqrt{2\times 3}}\right)(8p-8) + \ln\left(\frac{3+3}{2\sqrt{3\times 3}}\right)\left(3p^2-4p+1\right)\\
&= 0.1632p - 0.1632.
\end{aligned} \tag{3}
$$

□

3. Discussion and Graphical Representation

In this section, we present a graphical comparison of both benzenoid systems Z_p and R_p. The color red is fixed for the Z_p graph, while the color green is used for the R_p graph. This visual representation provides a clear comparison between the two systems, highlighting their similarities and differences.

From Figures 3–18, we can see that by fixing the values of structural parameters involved, we can control the irregularities of both Z_p and R_p. This is an important observation as it allows us to tailor the properties of these systems to suit specific applications. Furthermore, the graphical comparison in Figure 3 highlights the fact that different irregularities behave differently. Some irregularities in Z_p increase faster than those in R_p, while others do not increase faster. This is important because it suggests that the behavior of a particular irregularity is dependent on the specific parameters of the system under study. By carefully choosing these parameters, we can optimize the behavior of the system with respect to a particular irregularity. Overall, the results presented in this section provide valuable insights into the behavior of benzenoid systems and may prove useful in the design of materials for various applications.

4. Conclusion

In this study, we have presented a comprehensive analysis of the irregularity indices of Z_p and R_p, which are two structurally complex systems. Our findings reveal that these systems exhibit a high degree of irregularity, and the calculated indices provide valuable insight into their nature. The obtained results can be applied in the quantitative structure-activity relationship modeling of various physical and chemical properties of these systems. Additionally, the graphical comparison between Z_p and R_p highlights the differences in their irregularity behaviors, which can aid in the further understanding and characterization of these structures. Overall, this work contributes to the growing body of literature on irregularity indices and their applications in chemical graph theory.

5. Future Directions

Here are some possible future directions based on the findings of this study:

(1) Investigating the relationship between irregularity indices and physical/chemical properties of Z_p and R_p: this can be done through quantitative structure-activity relationship (QSAR) modeling, which can help predict properties of these structures and guide the design of new molecules with desirable properties.

(2) Studying the effect of varying the structural parameters of Z_p and R_p on their irregularity indices: this can provide insights into the factors that contribute to the irregular nature of these structures and guide the design of new structures with desired irregularity properties.

(3) Exploring the application of irregularity indices in other types of networks, such as biological networks and social networks: the use of irregularity indices can help characterize the complex structure of these networks and guide the design of more efficient and robust systems.

(4) Developing new methods for calculating irregularity indices that can handle larger and more complex networks: this can help extend the application of irregularity indices to a wider range of structures and facilitate the study of their properties.

6. Limitations of the Used Method

(1) The method is limited to calculating only the sixteen irregularity indices and may not be applicable to other types of indices or measures of irregularity.

(2) The method relies on the assumption that the considered graphs have an irregular nature, which may not be true for all types of graphs.

(3) The method assumes that the structural parameters involved are the only factors affecting the irregularity

indices, while other factors, such as environmental conditions, may also play a role in determining the properties of the underlying structures.

(4) The method does not consider the dynamic nature of the underlying structures and may not be suitable for analyzing their behavior over time.

(5) The method may have limitations in its applicability to real-world systems, as the structures considered in the study are theoretical models and may not fully reflect the complexity of real-world systems.

7. Robustness of the Proposed Method

The proposed method for calculating irregularity indices can be easily applied to other graph structures beyond Z_p and R_p. Therefore, the method shows promising robustness and versatility in analyzing the irregularities of different types of graphs.

Data Availability

The data used to support the findings of this study are included within the article.

Conflicts of Interest

The authors declare that they have no conflicts of interest.

Authors' Contributions

All authors contributed equally to this study.

References

[1] A. El-Mesady, Y. S. Hamed, and H. Shabana, "On the decomposition of circulant graphs using algorithmic approaches," *Alexandria Engineering Journal*, vol. 61, no. 10, pp. 8263–8275, 2022.

[2] A. El-Mesady, Y. S. Hamed, and K. M. Abualnaja, "A novel application on mutually orthogonal graph squares and graph-orthogonal arrays," *AIMS Mathematics*, vol. 7, no. 5, pp. 7349–7373, 2022.

[3] A. El-Mesady, O. Bazighifan, and S. S. Askar, "A novel approach for cyclic decompositions of balanced complete bipartite graphs into infinite graph classes," *Journal of Function Spaces*, vol. 2022, Article ID 9308708, 12 pages, 2022.

[4] F. M. Brückler, T. Doşlic, A. Graovac, and I. Gutman, "On a class of distance-based molecular structure descriptors," *Chemical Physics Letters*, vol. 503, no. 4-6, pp. 336–338, 2011.

[5] H. Gonzalez-Diaz, S. Vilar, L. Santana, and E. Uriarte, "Medicinal chemistry and bioinformatics-current trends in drugs discovery with networks topological indices," *Current Topics in Medicinal Chemistry*, vol. 7, no. 10, pp. 1015–1029, 2007.

[6] H. Hosoya, K. Hosoi, and I. Gutman, "A topological index for the totalp-electron energy," *Theoretica Chimica Acta*, vol. 38, no. 1, pp. 1–9, 1975.

[7] D. Vukicevic and A. Graovac, "Valence connectivity versus Randic, Zagreb and modified Zagreb index: a linear algorithm to check discriminative properties of indices in acyclic molecular graphs," *Croatica Chemica Acta*, vol. 77, no. 3, pp. 501–508, 2004.

[8] A. Milicevic, S. Nikolic, and N. Trinajstic, "On reformulated Zagreb indices," *Molecular Diversity*, vol. 8, no. 4, pp. 393–399, 2004.

[9] C. K. Gupta, V. Lokesha, S. B. Shwetha, and P. S. Ranjini, "On the symmetric division deg index of graph," *Southeast Asian Bulletin of Mathematics*, vol. 40, no. 1, 2016.

[10] O. Favaron, M. Mah'eo, and J. F. Sacl'e, "Some eigenvalue properties in graphs (conjectures of Graffiti II)," *Discrete Mathematics*, vol. 111, no. 1-3, pp. 197–220, 1993.

[11] T. R'eti, R. Sharafdini, A. Dregelyi-Kiss, and H. Haghbin, "Graph irregularity indices used as molecular descriptors in QSPR studies," *MATCH Commun. Math. Comput. Chem*, vol. 79, pp. 509–524, 2018.

[12] Y. Liu, A. Siddiqa, Y. M. Chu, M. Azam, M. A. R. Basra, and A. U. Rehman Virk, "Irregularity measures for Benzene ring embedded in P-type surface," *Mathematical Problems in Engineering*, vol. 2020, Article ID 2462530, 13 pages, 2020.

[13] A. T. Balaban, "Highly discriminating distance-based topological index," *Chemical Physics Letters*, vol. 89, no. 5, pp. 399–404, 1982.

[14] S. M. Hosamani, V. Lokesha, I. N. Cangul, and K. M. Devendraiah, "On certain topological indices of the derived graphs of subdivision graphs," *TWMS Journal of Applied and Engineering Mathematics*, vol. 6, no. 2, p. 324, 2016.

[15] A. El-Mesady, O. Bazighifan, and Q. Al-Mdallal, "On infinite circulant-balanced complete multipartite graphs decompositions based on generalized algorithmic approaches," *Alexandria Engineering Journal*, vol. 61, no. 12, pp. 11267–11275, 2022.

[16] A. El-Mesady and O. Bazighifan, "Decompositions of circulant-balanced complete multipartite graphs based on a novel labelling approach," *Journal of Function Spaces*, vol. 2022, Article ID 2017936, 17 pages, 2022.

[17] A. Ali, W. Nazeer, M. Munir, and S. Min Kang, "M-polynomials and topological indices of zigzag and rhombic benzenoid systems," *Open Chemistry*, vol. 16, no. 1, pp. 73–78, 2018.

[18] Y. Chel Kwun, M. A. Zahid, W. Nazeer, A. Ali, M. Ahmad, and S. M. Kang, "On the zagreb polynomials of benzenoid systems," *Open Physics*, vol. 16, no. 1, pp. 734–740, 2018.

[19] N. Idrees, F. Hussain, and A. Sadiq, "Topological properties of benzenoid graphs," *University Politehnica of Bucharest Scientific Bulletin Series B-Chemistry and Materials Science*, vol. 80, no. 1, pp. 145–156, 2018.

[20] M. A. Mohammed, R. S. Haoer, A. Ali, M. Ahmad, M. R. Farahani, and S. Nazeer, "Redefined zagreb indices of rhombic, triangular, hourglass and jagged-rectangle benzenoid systems," *Proyecciones (Antofagasta)*, vol. 39, no. 4, pp. 851–867, 2020.

[21] M. O'Keeffe, G. B. Adams, and O. F. Sankey, "Predicted new low energy forms of carbon," *Physical Review Letters*, vol. 68, no. 15, pp. 2325–2328, 1992.

[22] M. V. Diudea, *Nanostructures: Novel Architecture*, Nova Publishers, Hauppauge, NY, USA, 2005.

[23] M. V. Diudea and C. L. Nagy, *Periodic Nanostructures*, Springer Science & Business Media, Heidelberg, Germany, 2007.

[24] K. Y. Amsharov and M. A. Jansen, "A C_{78} fullerene Precursor: toward the direct synthesis of higher fullerenes," *Journal of Organic Chemistry*, vol. 73, no. 7, pp. 2931–2934, 2008.

[25] Y. Ma, B. Ma, Y. Shang et al., "Flavonoid-rich ethanol extract from the leaves of Diospyros kaki attenuates cognitive deficits, amyloid-beta production, oxidative stress, and neuroinflammation in APP/PS1 transgenic mice," *Brain Research*, vol. 1678, no. 1, pp. 85–93, 2018.